



Synthesis and characterizations of $(\text{In}_{0.90}\text{Sn}_{0.05}\text{Ni}_{0.05})_2\text{O}_3$ nanoparticles using solid state reaction method

S. Harinath Babu, N. Sai Krishna, S. Kaleemulla, N. Madhusudhana Rao, M. Kuppan, C. Krishnamoorthi, Girish M. Joshi, and G. A. Basheed

Citation: [AIP Conference Proceedings](#) **1731**, 120003 (2016); doi: 10.1063/1.4948075

View online: <http://dx.doi.org/10.1063/1.4948075>

View Table of Contents: <http://scitation.aip.org/content/aip/proceeding/aipcp/1731?ver=pdfcov>

Published by the [AIP Publishing](#)

Articles you may be interested in

[Raman and FT-IR studies of \$\(\text{In}_{0.90}\text{Sn}_{0.05}\text{Fe}_{0.05}\)_2\text{O}_3\$ nanoparticles](#)

AIP Conf. Proc. **1731**, 140008 (2016); 10.1063/1.4948174

[Structural, optical and magnetic properties of \$\(\text{In}_{0.90}\text{Sn}_{0.05}\text{Cu}_{0.05}\)_2\text{O}_3\$ nanoparticles](#)

AIP Conf. Proc. **1731**, 130005 (2016); 10.1063/1.4948111

[Structure and multiferroic properties of \$\text{Bi}\(1-x\)\text{Dy}_x\text{Fe}_{0.90}\text{Mg}_{0.05}\text{Ti}_{0.05}\text{O}_3\$ solid solution](#)

J. Appl. Phys. **113**, 054102 (2013); 10.1063/1.4790326

[Effects of \$\text{SrRuO}_3\$ buffer layer thickness on multiferroic \$\(\text{Bi}_{0.90}\text{La}_{0.10}\)\(\text{Fe}_{0.95}\text{Mn}_{0.05}\)\text{O}_3\$ thin films](#)

J. Appl. Phys. **106**, 054115 (2009); 10.1063/1.3213335

[Magnetic behavior of \$\(\text{Fe}_{0.90}\text{Cr}_{0.03}\text{Ni}_{0.07}\)_2\text{P}\$ and \$\(\text{Fe}_{0.90}\text{Cr}_{0.05}\text{Ni}_{0.05}\)_2\text{P}\$](#)

J. Appl. Phys. **73**, 5701 (1993); 10.1063/1.353596

Synthesis and Characterizations of $(\text{In}_{0.90}\text{Sn}_{0.05}\text{Ni}_{0.05})_2\text{O}_3$ Nanoparticles Using Solid State Reaction Method

S. Harinath Babu^a, N. Sai Krishna^a, S. Kaleemulla^{a*}, N. Madhusudhana Rao^a, M. Kuppan^a, C. Krishnamoorthi^a, Girish M. Joshi^a, G.A. Basheed^b

^aThin Films Laboratory, School of Advanced Sciences, VIT University, Vellore – 632 014, Tamilnadu, India

^bCSIR-National Physical Laboratory, Dr. K. S. Krishnan Road, New Delhi, India

*Email: skaleemulla@gmail.com

Abstract: ITO ($\text{In}_{0.95}\text{Sn}_{0.05}$)₂O₃ and Ni doped ITO ($\text{In}_{0.90}\text{Sn}_{0.05}\text{Ni}_{0.05}$)₂O₃ nanoparticles (NPs) were synthesized by solid state reaction method and subjected to study their structural, optical and magnetic properties. The NPs had a size distribution in the range of 40 nm and were identified as the bcc cubic In₂O₃ by X-ray diffraction (XRD). Optical properties of the samples were studied using UV-Vis-NIR spectrophotometer. Magnetic measurements were carried out at room temperature and at 100 K using vibrating sample magnetometer and found that the ITO nanoparticles were ferromagnetic in nature at room temperature. The strength of the magnetization decreased in ITO nanoparticles when the magnetic measurements carried out at 100 K.

Keywords: ITO, Dilute magnetic semiconductors, Ferromagnetic material.

PACS: 73.50.Td, 75.50.Pp, 75.47.Lx, 75.50.Dd

INTRODUCTION

In recent years, oxide based diluted magnetic semiconductors (O-DMSs) have become the subject of an intensive interest for fundamental scientific research because of the possibility of manipulating both charge and spin degree of freedom in a single semiconductor material. These O-DMSs materials are the most promising candidates because of their potential use in future spintronic devices such as optoelectronics, spin logic, microwave and non-volatile storage devices [1,2]. Intensive research work had been carried out on optical and electrical properties of ITO, but less work has been reported on magnetic properties of ITO and doped ITO nanoparticles. Ni doped ITO thin films were prepared using electron beam evaporation technique and studied the role of Ni on magnetic properties of the films [3]. However, the origin of ferromagnetism in transition metal ions doped In₂O₃ have still been controversial. Hence an attempt was made in the present study for the synthesis and characterization of undoped and Ni doped ITO nanoparticles using solid state reaction.

EXPERIMENTAL

The ITO ($\text{In}_{0.95}\text{Sn}_{0.05}$)₂O₃ and Ni doped ITO ($\text{In}_{0.90}\text{Sn}_{0.05}\text{Ni}_{0.05}$)₂O₃ nanoparticles were synthesized by standard solid state reaction method. In a typical synthesis, commercially available In₂O₃, SnO₂ and NiO (Sigma-Aldrich, 99.999% pure) powders were mixed in desired ratios using Agate mortar and pestle and ground thoroughly for 16 hours. The ground fine stoichiometric fine powder samples were loaded into a small one end closed quartz tube of diameter 10 mm and length 10 cm, which was then enclosed by a bigger quartz tube of diameter of 2.5 cm and length of 75 cm. The structural, optical and magnetic properties of the prepared samples were studied using XRD, UV-Vis spectrophotometer, Vibrating sample magnetometer, respectively.

RESULTS AND DISCUSSION

Structural Properties

Fig. 1 shows the X-ray diffraction patterns of ($\text{In}_{0.90}\text{Sn}_{0.05}\text{Ni}_{0.05}$)₂O₃. The XRD patterns conformed that the impurity phases were not

present in $(\text{In}_{0.90}\text{Sn}_{0.05}\text{Ni}_{0.05})_2\text{O}_3$ nanoparticles. The diffraction peaks such as (211), (2 2 2), (4 0 0), (411), (3 3 2), (4 3 1), (5 2 1), (4 4 0), (4 3 3), (6 11), (5 41), (6 2 2), (6 3 1), (4 4 4), (5 4 3), (6 4 0), (7 2 1) and (6 4 2) were found in $(\text{In}_{0.90}\text{Sn}_{0.05}\text{Ni}_{0.05})_2\text{O}_3$ nanoparticles among which (2 2 2) peak was predominant. All the indexed peaks exactly coincided with the cubic structure of In_2O_3 (JCPDS No. #06-0416). The crystallite size was calculated using Scherer's relation and found that it was about 40 nm.

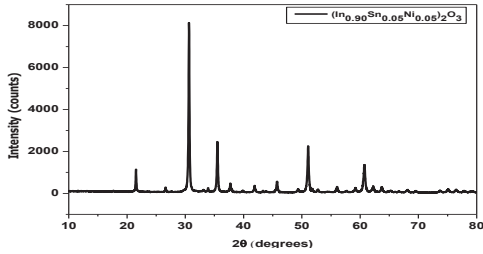


FIGURE 1. X-ray diffraction patterns of $(\text{In}_{0.90}\text{Sn}_{0.05}\text{Ni}_{0.05})_2\text{O}_3$ nanoparticles.

Optical Properties

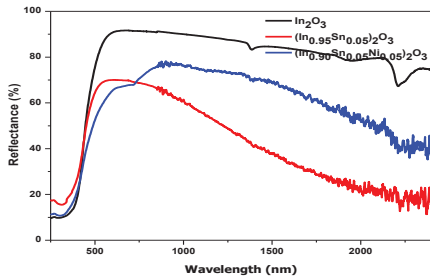


FIGURE 2. Reflectance spectra of In_2O_3 , $(\text{In}_{0.95}\text{Sn}_{0.05})_2\text{O}_3$ and $(\text{In}_{0.90}\text{Sn}_{0.05}\text{Ni}_{0.05})_2\text{O}_3$ nanoparticles.

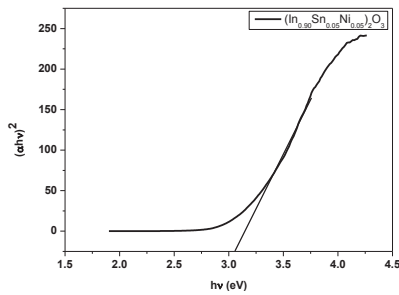


FIGURE 3. Plot of $(ah\nu)^2$ versus $h\nu$ of the $(\text{In}_{0.90}\text{Sn}_{0.05}\text{Ni}_{0.05})_2\text{O}_3$ nanoparticles.

Fig. 2 shows the diffused reflectance spectra of the In_2O_3 , $(\text{In}_{0.95}\text{Sn}_{0.05})_2\text{O}_3$ and $(\text{In}_{0.90}\text{Sn}_{0.05}\text{Ni}_{0.05})_2\text{O}_3$ nanoparticles recorded in the wavelength range from 200 nm to 2400 nm. In addition to reflectance spectra, absorption spectra was also estimated (not shown here) for calculating the optical band gap of the

$(\text{In}_{0.90}\text{Sn}_{0.05}\text{Ni}_{0.05})_2\text{O}_3$ nanoparticles. The optical band gap was estimated using the Tauc relation [4]. An optical band gap of 3.06 eV was found for the $(\text{In}_{0.95}\text{Sn}_{0.05}\text{Ni}_{0.05})_2\text{O}_3$ nanoparticles as shown in Fig. 3. A decrease in optical band gap was observed by doping Ni into the ITO host material. The band gap of 3.14 eV was found for the undoped ITO $(\text{In}_{0.95}\text{Sn}_{0.05})_2\text{O}_3$ nanoparticles.

Magnetic Properties

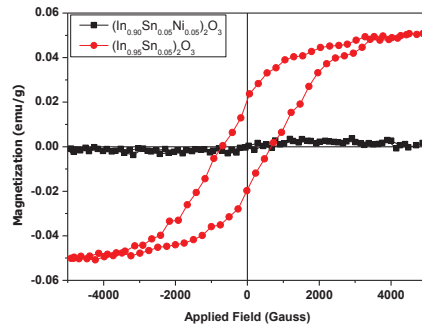


FIGURE 4. Magnetic hysteresis loops (M-H) of ITO and Ni doped ITO nanoparticles at room temperature.

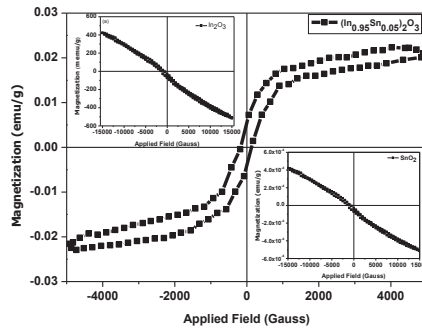


FIGURE 5. Magnetic hysteresis loops (M-H) of ITO nanoparticles at 100 K. Top and bottom inset of the figure shows the diamagnetic nature of In_2O_3 and SnO_2 .

Fig. 4 shows magnetic hysteresis loops (M-H) of ITO $(\text{In}_{0.95}\text{Sn}_{0.05})_2\text{O}_3$ and Ni doped ITO $(\text{In}_{0.90}\text{Sn}_{0.05}\text{Ni}_{0.05})_2\text{O}_3$ nanoparticles at room temperature. The pure In_2O_3 and SnO_2 exhibited diamagnetic behaviour whereas the $(\text{In}_{0.95}\text{Sn}_{0.05})_2\text{O}_3$ exhibited ferromagnetism at room temperature and the strength of magnetization decreased in case of $(\text{In}_{0.90}\text{Sn}_{0.05}\text{Ni}_{0.05})_2\text{O}_3$ nanoparticles. Our earlier studies confirmed the diamagnetism and room temperature ferromagnetism undoped and transition metal doped In_2O_3 , SnO_2 in powder form as shown in top and bottom inset of the Fig. 4. And reported that the observed room temperature ferromagnetism was due to oxygen vacancies [5-8]. The hysteresis loop shows a high coercive field (H_c) of 683 G. The observed magnetic moment is almost equal to that of magnetic moment of Ni doped In_2O_3 nanoparticles prepared by solid state

synthesis route method observed by Peleckis et al [9]. The strength of magnetization decreased for $(\text{In}_{0.90}\text{Sn}_{0.05}\text{Ni}_{0.05})_2\text{O}_3$ nanoparticles. The samples exhibited the saturation magnetic moment of 0.05 emu/g, coercivity of 683G and retentivity of 0.02 emu/g, respectively.

Fig.5 shows the M-H curve of ITO nanoparticles at 100 K. From the figure it is clear that the saturation magnetic moment decreased at lower temperature which may be due to antiferromagnetic or ferrimagnetism developed at lower temperatures. Room temperature ferromagnetism was also found in nanoparticles of nonmagnetic oxides such as CeO_2 , Al_2O_3 , ZnO , In_2O_3 and SnO_2 [10]; however, the corresponding bulk samples obtained by sintering the nanoparticles at high temperatures in air or oxygen became diamagnetic. The origin of ferromagnetism in these nanoscale materials is assumed to be the exchange interactions between localized electron spin moments resulting from the oxygen vacancies [11]. Recent calculations also indicated that surface ferromagnetic states and spin polarization could produce vacancies on the surface of In_2O_3 and ITO [12]. A magnetic moment of 5×10^{-6} emu, 1×10^{-8} emu was observed in polycrystalline bulk and thin films of ITO [13]. The observed magnetic moment in the present study is higher than that of magnetic moment observed in polycrystalline bulk ITO nanoparticle prepared from solid state synthesis method. The less magnetic moment in polycrystalline ITO may be due to sintering of the samples in air at different higher temperatures. Further it was found that the bulk ITO samples were paramagnetic at low temperatures and diamagnetic at higher temperature. In the present study the samples were sintered in vacuum which may produce oxygen vacancies. Room temperature ferromagnetism was also observed in Fe-doped ITO thin films and concluded that the observed ferromagnetism is due to oxygen vacancies [14]. Hence in the present studies, it is confirmed that the observed ferromagnetism is intrinsic rather than any impurities. After doping the ITO with other transition metal dopants, the strength of magnetization decreased to a large extent.

CONCLUSION

The ITO $(\text{In}_{0.95}\text{Sn}_{0.05})_2\text{O}_3$ and Ni doped ITO $(\text{In}_{0.90}\text{Sn}_{0.05}\text{Ni}_{0.05})_2\text{O}_3$ nanoparticles were prepared using standard solid state reaction method and studied the structural, optical properties by XRD, diffused reflectance spectrometers respectively. The structural properties confirmed that the $(\text{In}_{0.90}\text{Sn}_{0.05}\text{Ni}_{0.05})_2\text{O}_3$ nanoparticles were cubic in structure without any secondary phases. The pure In_2O_3 , SnO_2 exhibited diamagnetic behavior whereas $(\text{In}_{0.95}\text{Sn}_{0.05})_2\text{O}_3$ nanoparticles exhibited

ferromagnetism at room temperature and at 100 K. A decrease in strength of magnetization was observed in $(\text{In}_{0.90}\text{Sn}_{0.05}\text{Ni}_{0.05})_2\text{O}_3$ nanoparticles.

ACKNOWLEDGMENTS

Authors are thankful to VIT-SIF for providing XRD and diffused reflectance spectra (DRS) facilities.

REFERENCES

1. S.A. Wolf, D.D. Awschalom, R.A. Buhrman, J.M. Daughton, S. von Molnar, M.L. Roukes, A.Y. Chtchelkanova, and D.M. Treger, *Science* **294**, 1488-1495 (2001).
2. H. Ohno, H. Munekata, T. Penney, S. V. Molnar and L.L. Chang, *Phys. Rev. Lett.* **68**, 2664-7 (1992).
3. F. Ay, B. Aktaş, R.I. Khaibullin, V.I. Nuzhdin and B.Z. Rameev, *J. Magn. Mater.* **375**, 129-135 (2015).
4. J. Tauc, *Amorphous and Liquid Semiconductors*. Plenum Press, New York (1974).
5. N. Sai Krishna, S. Kaleemulla, N. Madhusudhana Rao, M. Kuppan M. Rigana Begam and D. Sreekantha Reddy, *Mater. Sci. Semi. Proc.* **18**, 22-27 (2014).
6. N. Sai Krishna, N. Madhusudhana Rao, S. Kaleemulla, C. Krishnamoorthi, M. Rigana Begam, M. Kuppan, D. Sreekantha Reddy and I. Omkaram, *Mater. Res. Bull.* **61**, 486-491 (2015).
7. M. Kuppan, S. Kaleemulla, N. Madhusudhana Rao, N. Sai Krishna, M. Rigana Begam and D. Sreekantha Reddy, *J. Supercond. Novel Magn.* **27**, 1315-1321 (2014).
8. M. Kuppan, S. Kaleemulla, N. Sai Krishna, N. Madhusudhana Rao, M. Rigana Begam and M. Shobana, *Adv. Condens. Matt. Phys.* **284237**, 1-5 (2014).
9. G. Peleckis, X. Wang and S.X. Dou, *Appl. Phys. Lett.* **89**, (2006) 022501-3.
10. A. Sundaresan, R. Bhargavi, N. Rangarajan, U. Siddesh and C.N.R. Rao, *Phys. Rev.* **B74**, 161306-4 (2006).
11. C.D. Pemmaraju and S. Sanvito, *Phys. Rev. Lett.* **94**, 217205-217208 (2005).
12. H.S. Majumdar, S. Majumdar, D. Tobjork and R. Osterbacka, *Synthetic Mater.* **160**, 303-306 (2010).
13. B. Xia, Y. Wu, H.W. Ho, C. Ke, W.D. Song, C.H.A. Huan, J.L. Kuo, W.G. Zhu and L. Wang, *Physica B* **406**, 3166-3169 (2011).
14. X. Pengfei, C. Yanxu and S. Shaohua, *J. Semi. Cond.* **34**, 023002-4 (2013).